NASA TECHNICAL NOTE

NASA TN D-7510

NASA TN D-7510

COMPARISON OF MEASURED AND CALCULATED VELOCITY PROFILES OF A LAMINAR INCOMPRESSIBLE FREE JET AT LOW REYNOLDS NUMBERS

by George C. Greene

Langley Research Center
Hampton, Va. 23665

NATIONAL AERONAUTICS AND SPACE ADMINISTRATION • WASHINGTON, D. C. • MAY 1974

1. Report No.	2. Government Accession No.	3. Recipient's Catalog No.
NASA TN D-7510		

4. Title and Subtitle	5. Report Date
COMPARISON OF MEASURED AND CALCULATED VELOCITY PROFILES OF A LAMINAR INCOMPRESSIBLE FREE JET AT LOW REYNOLDS NUMBERS	May 1974
	6. Performing Organization Code

7. Author(s)	8. Performing Organization Report No.
George C. Greene	L-9277
	10. Work Unit No.
	501-04-01-01

9. Performing Organization Name and Address	11. Contract or Grant No.
NASA Langley Research Center Hampton, Va. 23665	
	13. Type of Report and Period Covered
	Technical Note

12. Sponsoring Agency Name and Address	14. Sponsoring Agency Code
National Aeronautics and Space Administration Washington, D.C. 20546	

15. Supplementary Notes

The information presented herein was included in a thesis, entitled "An Investigation of a Free Jet at Low Reynolds Numbers," submitted in partial fulfillment of the requirements for the degree of Master of Engineering, Old Dominion University, Norfolk, Virginia, August 1973.

16. Abstract

This paper presents a comparison of the measured and calculated velocity profiles of a laminar, incompressible, low Reynolds number jet. The experimental jet was produced by a "nozzle" which consists of a porous metal plate covering the end of a pipe. This nozzle produces a uniform exit velocity profile at Reynolds numbers well below those at which conventional contoured nozzles are completely filled by the boundary layer. A jet mixing analysis based on the boundary-layer equations accurately predicted the velocity field for each test condition. The Reynolds number based on nozzle diameter ranged from 50 to 1000 with jet exit velocity either 30 or 61 m/s (100 or 200 ft/sec).

17. Key Words (Suggested by Author(s))	18. Distribution Statement
Low Reynolds number nozzle Laminar flow nozzle	Unclassified – Unlimited STAR Category 12

19. Security Classif. (of this report)	20. Security Classif. (of this page)	21. No. of Pages	22. Price*
Unclassified	Unclassified	21	$3.00

*For sale by the National Technical Information Service, Springfield, Virginia 22151

COMPARISON OF MEASURED AND CALCULATED VELOCITY PROFILES OF A LAMINAR INCOMPRESSIBLE FREE JET AT LOW REYNOLDS NUMBERS*

By George C. Greene
Langley Research Center

SUMMARY

A comparison of the measured and calculated velocity profiles of a jet produced by a nozzle of unusual design is presented. The "nozzle," which was essentially a pipe capped with a porous metal plate, was used to generate a laminar, incompressible, low Reynolds number jet. A jet mixing analysis based on the boundary-layer equations was used for the flow-field calculations. Results are presented for nozzle Reynolds numbers from 50 to 1000 with nozzle velocities of either 30 or 61 m/s (100 or 200 ft/sec).

The porous-plate nozzle produced a reasonably uniform exit velocity profile over the range of Reynolds numbers investigated. This contrasts with a conventional contoured nozzle which has a large boundary layer at a Reynolds number of 1000 and is completely filled with boundary layer at Reynolds numbers on the order of 200. The jet mixing analysis accurately predicted the flow field over the entire Reynolds number range.

INTRODUCTION

In the past decade several methods of measuring the temperature of the Earth upper atmosphere have been developed. In one of these methods a small sounding rocket is used to carry an instrument package and parachute aloft. After ejection the instrument package descends through the atmosphere suspended beneath the parachute and telemeters temperature data to the ground. These temperature data must be corrected for several types of errors, one of which is aerodynamic heating. Correcting for aerodynamic heating requires that the recovery factor of the transducer be accurately known. Recovery factors for simple shapes are well documented in the literature for a wide range of flow conditions. However, for more complex geometries, the recovery factor must be determined experimentally.

---

*The information presented herein was included in a thesis, entitled "An Investigation of a Free Jet at Low Reynolds Numbers," submitted in partial fulfillment of the requirements for the degree of Master of Engineering, Old Dominion University, Norfolk, Virginia, August 1973.

In a typical experimental arrangement for determining the recovery factor, the temperature transducer is placed in a wind tunnel or jet of air to simulate the fall through the atmosphere. The flow Mach number (fall velocities are generally subsonic) and Reynolds number are duplicated to maintain the proper heat-transfer characteristics. However, for the very low Reynolds numbers required to duplicate the conditions in the upper atmosphere, conventional nozzles develop very thick boundary layers. This problem becomes serious at flow Reynolds numbers (based on the nozzle diameter and the density, velocity, and viscosity at the nozzle exit) of about 1000 and gets progressively worse until the entire nozzle is filled by the boundary layer at Reynolds numbers of about 200 (ref. 1).

Because of this Reynolds number limitation, a research program was initiated to develop a nozzle yielding a uniform exit velocity profile at low Reynolds numbers. In reference 1 some encouraging results from a test of a low Reynolds number, supersonic multinozzle were presented. This multinozzle consisted of 37 small nozzles in a 5-cm-diameter (2 in.) plate. This experiment met with only partial success in that a uniform velocity profile was not established until the flow had progressed many diameters downstream. This finding is in agreement with the results of references 2 and 3 for multinozzles operated at high Reynolds numbers.

In reference 4 it was postulated that a uniform flow could be established in a shorter distance if the multinozzle were made up of small closely spaced nozzles. In reference 5, multinozzles made of wire mesh were tested and were found to produce a reasonably uniform velocity profile almost immediately downstream of the nozzle exit. The nozzle used in the present study is similar to the wire-mesh nozzle and evolved from tests of various types of filter papers and screens. It was made from a porous plate of 0.3-cm-thick (0.125 in.) sintered stainless steel. This material is used commercially for filtration since it has a very small mesh size.

The purpose of this paper is to present measurements of the velocity field of the jet produced by this nozzle for Reynolds numbers based on nozzle diameter between 50 and 1000 and to compare these measured data with the results calculated from a boundary-layer type analysis.

SYMBOLS

Measurements and calculations were made in the U.S. Customary Units. They are presented herein in the International System of Units (SI) with equivalent values given parenthetically in U.S. Customary Units.

D	nozzle diameter, cm (in.)
M	Mach number
N_{Re}	Reynolds number based on diameter, $\rho uD/\mu$
p	pressure, Pa (mm Hg)
R	nozzle radius, cm (in.)
T	temperature, K (^{o}F)
u	velocity in the x-direction, m/s (ft/sec)
u_{max}	maximum jet velocity at a given value of x/R, m/s (ft/sec)
x,y,z	jet coordinates, cm (in.)
γ	ratio of specific heats
μ	coefficient of viscosity, Pa-s (slugs/ft-sec)
ρ	density, kg/m^3 (slugs/ft^3)

Subscripts:

e	conditions at $y = \infty$
i	impact tube conditions
t	stagnation conditions
∞	free-stream conditions

TEST APPARATUS AND PROCEDURE

Figure 1 shows a schematic diagram of the test apparatus used in this investigation. The porous-plate nozzle was bolted to the end of a 19.37-cm-diameter (7.626 in.) pipe which extended through the wall of a 17-m-diameter (55 ft) vacuum chamber. The porous-plate nozzle consisted of 5 layers of stainless-steel screen sintered to form a rigid plate 0.3 cm (0.125 in.) thick. The innermost screen had a mesh size of about 0.13 μm (5×10^{-6} in.). The outer screens had a larger mesh size to provide strength.

Outside the vacuum chamber, air was passed through a dryer, pressure regulator, vertical-tube flowmeter, and manual control valve into the nozzle pipe. The airstream

stagnation temperature was measured inside the nozzle pipe by using a shielded thermocouple. Downstream of the nozzle the flow Mach number was determined from pressure measurements.

The total pressure was determined from impact-tube measurements after applying a viscous correction. This correction was based on the data in reference 6 for an open-end impact tube of the type shown schematically in figure 2. A differential pressure transducer with a range of 0 to 1333 Pa (0 to 10 mm Hg) was used to measure the difference between the impact-tube pressure and the background ambient pressure. The background pressure was assumed to be the same as the static pressure inside the jet. The background pressure was measured at a point outside the jet near the nozzle exit with an absolute pressure transducer with a range of 0 to 1333 Pa (0 to 10 mm Hg). Both pressure transducers were kept in a controlled temperature environment to minimize temperature effects. The jet static temperature was calculated from the stagnation temperature and flow Mach number assuming adiabatic flow. The air density and viscosity were calculated from the perfect gas equation and the Sutherland viscosity formula (ref. 7), respectively.

Impact-pressure measurements were made by moving the impact tube with a remotely controlled, two-dimensional survey mechanism. The device was constructed and alined so that surveys could be made either axially along the nozzle center line or vertically along a nozzle radius. Calibrated potentiometers were used to indicate distances in each survey direction. The nozzle coordinate system is shown in figure 3.

Flow-field surveys were made at nozzle Reynolds numbers of 50, 100, 200, 600, and 1000. Nominal flow velocities were either 30 m/s (100 ft/sec) or 61 m/s (200 ft/sec). These velocities correspond to Mach numbers of 0.089 and 0.178 which were sufficiently low to insure essentially incompressible flow conditions. The Reynolds number was varied by changing the density of the air. The test conditions for each Reynolds number are listed in table I.

Before each test the static pressure transducer was compared with a reference transducer to check for zero drift. The differential pressure transducer used to measure the impact-tube pressure was checked for zero drift when the chamber was at the desired static pressure just prior to establishing the flow. The desired flow conditions were established based on the indicated dynamic pressure from the impact-tube measurement with precomputed viscous corrections. Preliminary surveys were made to establish the fact that the jet was axisymmetric. Surveys were then made from the jet center line outward along a radius at various positions along the jet axis. After a complete flow-field survey, the process was repeated for the next Reynolds number.

MEASUREMENT ACCURACY

An error estimate was made for each of the variables of interest. The errors in the measured quantities were determined directly from instrument characteristics. The errors in calculated quantities were estimated from the errors of each measured quantity in a root-sum-square manner. An error summary is presented in table II.

The total-temperature accuracy is based on the manufacturer's specifications for the thermocouple. The total-temperature error of ±1 K (±2° F) represents only 0.4 percent of the absolute temperature and is a relatively small error source.

The error in both the static pressure and the difference between the impact and static pressures is primarily due to instrument zero drift. The static pressure transducer was located in a small controlled environment chamber inside the large vacuum chamber. The transducer was not readily accessible for zero calibration since this required physically pumping the transducer to zero pressure. Just prior to each test, however, the static pressure was measured with both transducers and the reading of the static pressure transducer was corrected to the value indicated by the reference transducer. Zero check for the differential pressure transducer was done prior to each test just before flow conditions were established.

The error in measuring the survey probe position was estimated to be about ±0.08 cm (±0.03 in.), primarily due to gear backlash in the traversing mechanism. The error was estimated by clamping the probe in a fixed position and monitoring the position readout while turning the motor in either direction.

Table II also gives an error estimate for variables calculated from the primary measurements. The density error is based on a combination of the temperature and pressure errors through the perfect gas equation assuming that the gas constant is known. The viscosity error is based on the temperature error and the Sutherland viscosity equation given in reference 7.

The error in determining the flow velocity is based on a 10-percent uncertainty in the impact-tube viscous correction constant, the temperature error for determining the speed of sound, and the pressure errors for determining the Mach number. The error in the speed of sound is only ±0.2 percent with the ratio of specific heats and gas constant being known. The Mach number error in terms of the pressure ratio error is given by

$$\frac{\delta M}{M} = \frac{1 + \frac{\gamma - 1}{2} M^2}{\gamma M^2} \frac{\delta \frac{p_t}{p_\infty}}{p_t/p_\infty} \tag{1}$$

or, in terms of the measured quantities,

$$\frac{\delta M}{M} = \left(\frac{1 + \frac{\gamma - 1}{2} M^2}{\gamma M^2}\right)\left[1 - \left(1 + \frac{\gamma - 1}{2} M^2\right)^{\frac{-\gamma}{\gamma - 1}}\right]\left\{\left(\frac{\delta p_\infty}{p_\infty}\right)^2 + \left[\frac{\delta(p_t - p_\infty)}{p_t - p_\infty}\right]^2\right\}^{1/2} \tag{2}$$

The error in flow Reynolds number is simply the square root of the sum of the squares of the errors in density, viscosity, and velocity. The error in measuring probe diameter is included in the uncertainty of the impact-tube viscous correction.

JET FLOW-FIELD ANALYSIS

The jet flow field was analyzed by using the computer program described by Fox, Sinha, and Weinberger in reference 8. This program solved the equations for the conservation of mass, momentum, and energy (with boundary-layer assumptions) in the Von Mises plane using an implicit finite-difference numerical technique with free shear-flow boundary conditions.

The program is structured to calculate either jet or wake flow fields. All velocities are ratioed to an external velocity u_e, which for a wake flow is the free-stream velocity at the outer edge of the wake. However, for a jet flowing into a fluid at rest, u_e is zero and the nondimensional velocities would be infinite. This problem would normally be avoided by making u_e arbitrarily small since, as can be seen in figure 4.3 of reference 9, the solution is not very sensitive to changes in u_e. However, the numerical calculation step size depends on the Reynolds number of the external flow and hence on u_e. At low nozzle Reynolds numbers, small values of u_e produce prohibitively long run times. As a compromise, u_e was assumed to be 5 percent of the nozzle exit velocity for all calculations. This produced reasonable run times without introducing excessively large errors in the calculated velocity profiles.

Program inputs for starting the calculations are nondimensional velocity and temperature profiles at an initial station in the jet. The initial station was chosen to be the nozzle exit, and a uniform velocity and temperature profile were assumed to exist there. At the edge of the nozzle it was assumed that the velocity made a step change to the value of u_e. The ambient temperature outside the jet was assumed to be equal to the jet static temperature.

RESULTS AND DISCUSSION

Jet velocity profiles for nozzle Reynolds numbers between 50 and 1000 are presented in figures 4 to 8. Figure 4 shows the development of the velocity profiles in the

downstream direction for a nozzle Reynolds number of 1000. Velocity profiles are shown for three axial stations: $x/R = 1.0$, 2.5, and 7.0. For each velocity profile, the ratio of local velocity to the maximum jet velocity u/u_{max} was plotted against the nondimensional radial coordinate y/R. The symbols represent the measured data and the solid line represents the computed results. The measured and computed results are in good agreement except at $x/R = 7.0$, which was the maximum distance at which measurements were made. At this station, the calculated results predicted a slightly smaller potential core than was found experimentally. The calculated results indicate that the potential core extends to about $x/R = 30$ if the flow remains laminar.

Figure 5 shows a set of velocity profiles for a nozzle Reynolds number of 600. Again, u/u_{max} is plotted against y/R, for $x/R = 1.0$, 2.5, and 7.79. The agreement between calculated and measured results is good except at $x/R = 7.79$ where again the calculated results show a smaller potential core. The core is still large at this station and according to the analysis extends downstream to about $x/R = 20$.

Figure 6 shows typical velocity profiles for a nozzle Reynolds number of 200 where u/u_{max} is plotted against y/R for $x/R = 0.5$, 2.5, and 6.0. The agreement between measured and calculated results is very good at each station. The potential core extends downstream to about $x/R = 6$. At $x/R = 0.5$ and 2.5 there is a reasonably large region of uniform velocity. It should be noted that at Reynolds numbers of about 200, a conventional contoured nozzle would be nearly filled with boundary layer at the nozzle exit.

Figure 7 shows the calculated and measured flow-field data for a nozzle Reynolds number of 100 with u/u_{max} plotted against y/R for $x/R = 0.5$, 2.0, and 2.5. At $x/R = 0.5$ and 2.0 there still remains a relatively large area of uniform flow.

Figure 8 shows the velocity profiles for a nozzle Reynolds number of 50, the lowest Reynolds number at which flow surveys were made. In this figure, u/u_{max} is again plotted against y/R for $x/R = 1.0$, 2.5, and 5.0. The potential core extends downstream to only about $x/R = 1.0$. The calculated results, which agree with the data very well further downstream, indicate that there is still a large region of uniform flow just downstream of the nozzle. For example, at $x/R = 0.5$, the calculated results indicate that the potential core extends out radially to $y/R = 0.5$.

As mentioned earlier, the agreement between the measured and calculated results is very good and would be even better if the initial velocity profile which is used to start the flow-field calculations was more accurate. It was assumed that at the nozzle exit the velocity was uniform across the entire nozzle with a step change at the edge of the nozzle. However, the data indicate that the velocity was not quite uniform across the nozzle, especially at the higher Reynolds numbers. These errors enter the calculations and produce a large part of the discrepancies.

Another problem is choosing the value of velocity used for the background gas. At low Reynolds numbers, small values of the background gas velocity u_e produce prohibitively long run times. In this study, u_e was taken to be 5 percent of the jet exit velocity for all calculations. This produced reasonable run times without introducing excessively large errors in the calculated velocity profiles as demonstrated by figure 9.

In figure 9, the 0.5-velocity radius (value of y/R at which $u/u_{max} = 0.5$) is plotted against x/R for Reynolds numbers of 1000, 600, 200, 100, and 50. The 0.5-velocity radius is a measure of the jet width and its change in the downstream direction is a measure of the jet spreading rate. The good agreement between measured and calculated results is an indication that the value chosen for u_e is reasonable.

CONCLUSIONS

A comparison of the measured and calculated velocity profiles of a laminar, incompressible free jet is presented. The experimental jet was produced by a nozzle which consisted of a porous metal plate covering the end of a pipe. From results presented for nozzle Reynolds numbers between 50 and 1000, the following conclusions can be drawn:

1. The porous-plate nozzle produced a reasonably uniform velocity profile over a range of Reynolds numbers from 1000 down to 50. This contrasts with a conventional contoured nozzle which would have a large boundary layer at a Reynolds number of 1000 and would be completely filled with boundary layer at Reynolds numbers on the order of 200.

2. A conventional boundary-layer type analysis was sufficient to accurately calculate velocity profiles and spreading rate of the jet for nozzle Reynolds numbers as low as 50.

Langley Research Center,
National Aeronautics and Space Administration,
Hampton, Va., January 24, 1974.

REFERENCES

1. Stalder, Jackson R.: The Use of Low-Density Wind Tunnels in Aerodynamic Research. Rarefied Gas Dynamics, Vol. 3, F. M. Devienne, ed., Pergamon Press, Inc., 1960, pp. 1-20.

2. Reshotko, Eli; and Haefeli, Rudolph C.: Investigation of Axially Symmetric and Two-Dimensional Multinozzles for Producing Supersonic Streams. NACA RM E52H28, 1952.

3. Wagner, Jerry L.: A Cold Flow Field Experimental Study Associated With a Two-Dimensional Multiple Nozzle. NOLTR 71-78, U.S. Navy, July 1, 1971.

4. Lange, A. H.; and Walter, L. W.: Pressure and Temperature Measurements of the Flow Produced by a 12 × 12 cm Grating Nozzle. NAVORD Rep. 2678, U.S. Navy, Jan. 28, 1953.

5. Gould, Lawrence I.: Preliminary Investigation of the Supersonic Flow Field Downstream of Wire-Mesh Nozzles in a Constant-Area Duct. NACA RM E51F25, 1951.

6. Sherman, F. S.: New Experiments on Impact-Pressure Interpretation in Supersonic and Subsonic Rarefied Air Streams. NACA TN 2995, 1953.

7. Anon.: Equations, Tables, and Charts for Compressible Flow. NACA Rep. 1135, 1953.

8. Fox, Herbert; Sinha, Ram; and Weinberger, Lawrence: An Implicit Finite Difference Solution for Jet and Wake Problems. Astronaut. Acta, vol. 17, no. 3, June 1972, pp. 265-278.

9. Pai, Shih-I: Fluid Dynamics of Jets. D. Van Nostrand Co., Inc., c.1954, p. 82.

TABLE I.- TEST CONDITIONS

Nozzle Reynolds number	Static pressure		Dynamic pressure		$p_i - p_\infty$		Nominal velocity	
	Pa	mm Hg	Pa	mm Hg	Pa	mm Hg	m/s	ft/sec
50	13.3	0.1	0.07	0.00055	0.25	0.00186	30	100
100	26.7	.2	.15	.00109	.32	.00241	30	100
200	26.7	.2	.59	.00442	.94	.00706	61	200
600	80.0	.6	1.77	.0133	2.12	.0159	61	200
1000	133.3	1.0	2.95	.0221	3.30	.0247	61	200

TABLE II.- MEASUREMENT ACCURACY

Variable	Error magnitude	Comments
T_t	±1 K (±2° F)	Manufacturer's specification
p_∞	±0.4 Pa ($\pm 3 \times 10^{-3}$ mm Hg)	Short term accuracy; errors due primarily to zero drift; zero checked before each test
$p_i - p_\infty$	±0.01 Pa ($\pm 1 \times 10^{-4}$ mm Hg)	
x,y	±0.08 cm (±0.03 in.)	Primarily gear backlash in survey device
ρ	±0.5% to ±3.0%	Error is function of static pressure; derived from temperature and pressure errors and perfect gas relation $\frac{\delta\rho}{\rho} = \sqrt{\left(\frac{\delta p}{p}\right)^2 + \left(\frac{\delta T}{T}\right)^2}$
μ	±0.3%	Based on temperature error and Sutherland's viscosity equation
u	±1% to ±7%	Based on Mach number error which is a function of the pressure errors (see text) and a 10% uncertainty in the viscous correction constant
N_{Re}	1.3% to 8%	Based on errors in ρ, u, and μ $\frac{\delta N_{Re}}{N_{Re}} = \sqrt{\left(\frac{\delta\rho}{\rho}\right)^2 + \left(\frac{\delta u}{u}\right)^2 + \left(\frac{\delta\mu}{\mu}\right)^2}$

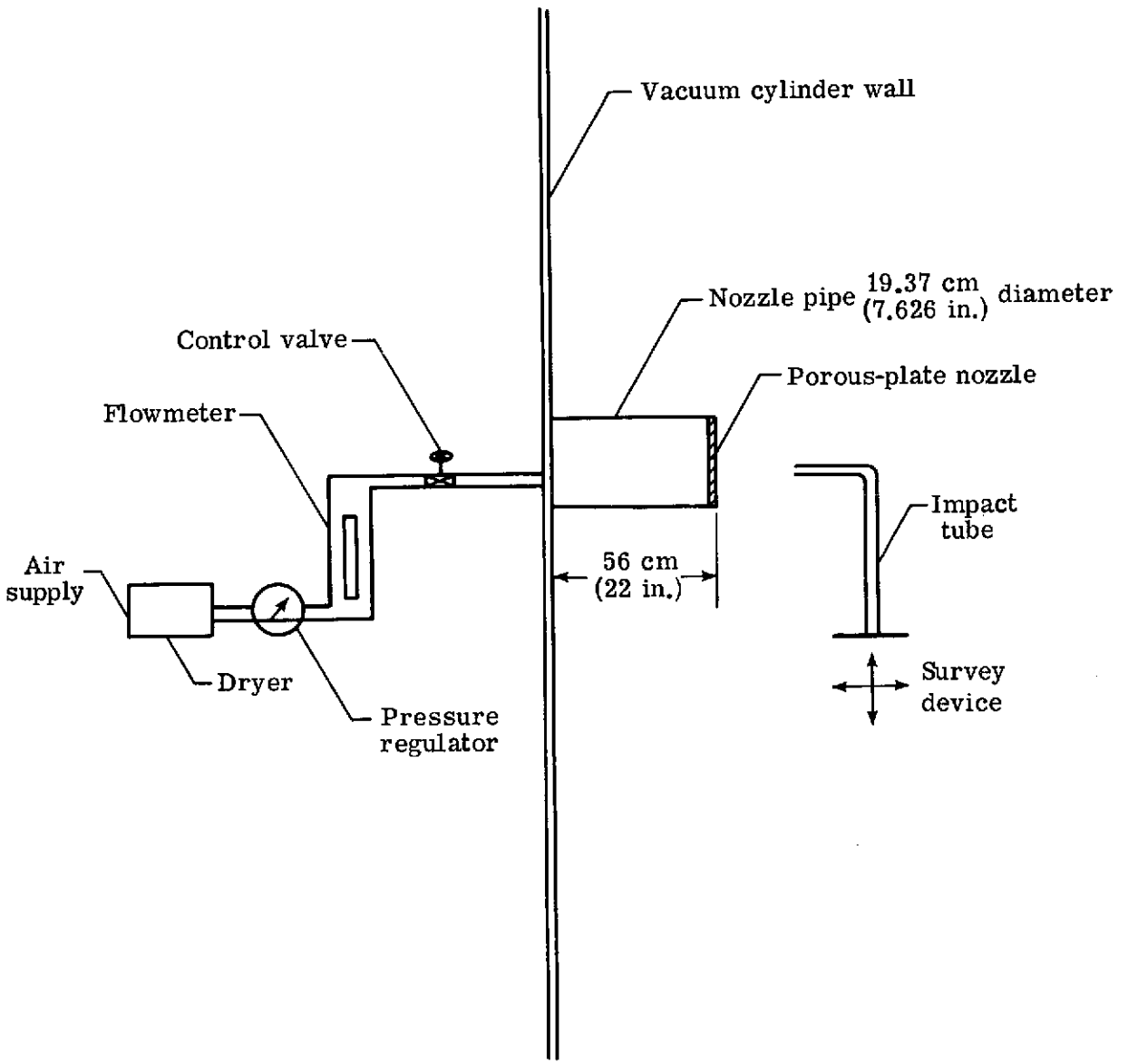

Figure 1.- Schematic diagram of test apparatus.

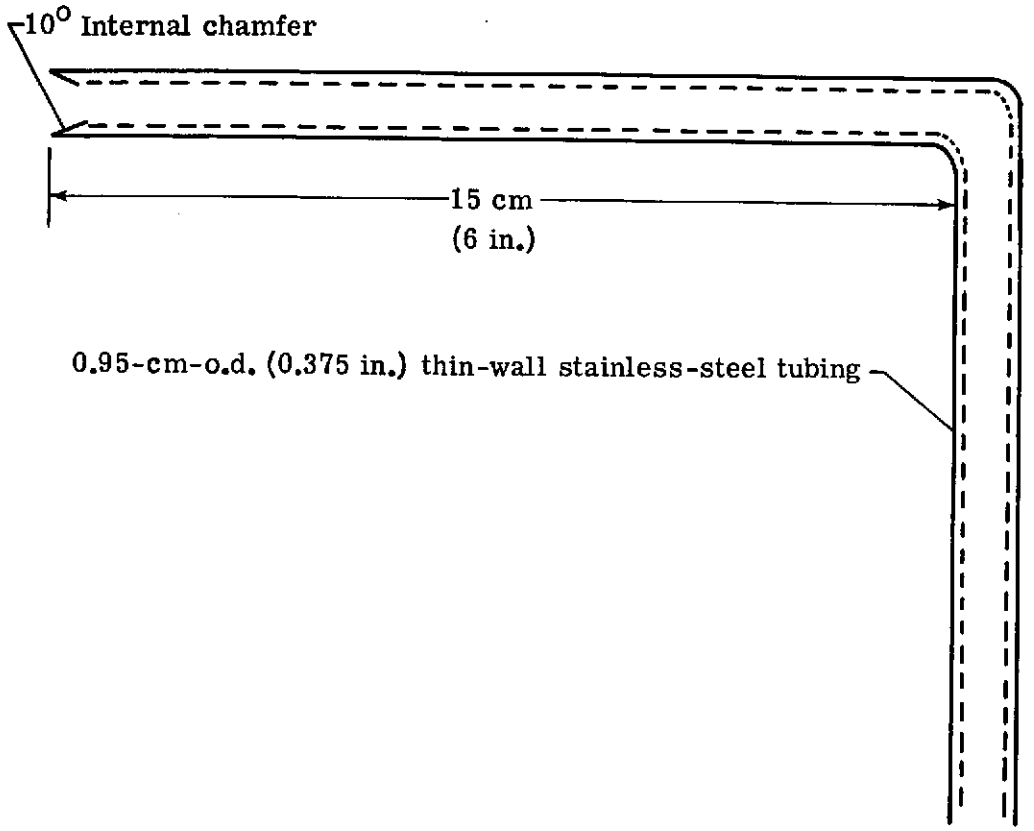

Figure 2.- Schematic diagram of impact tube.

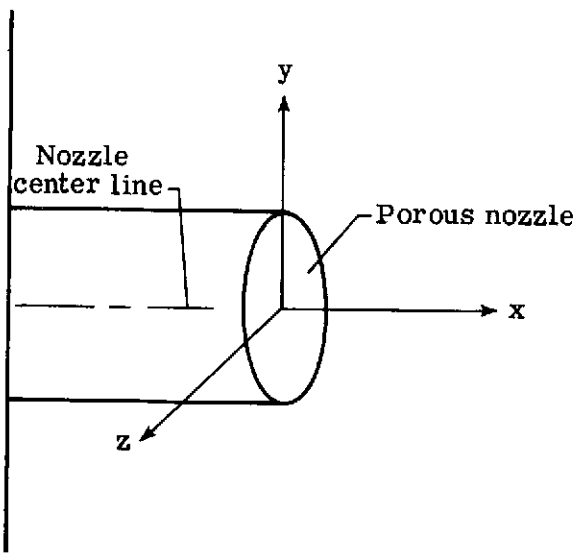

Figure 3.- Nozzle coordinate system.

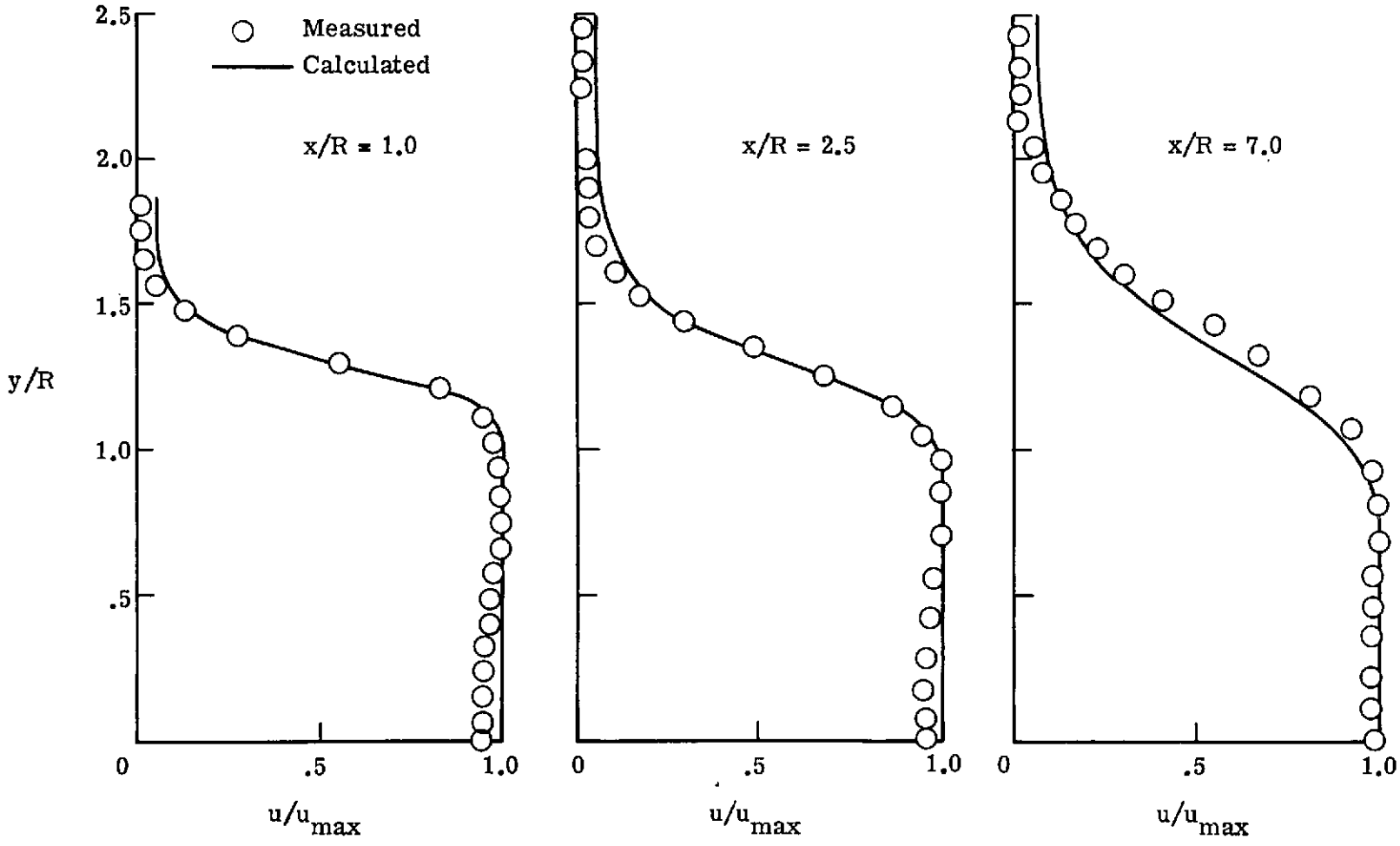

Figure 4.- Jet velocity profiles for Reynolds number of 1000.

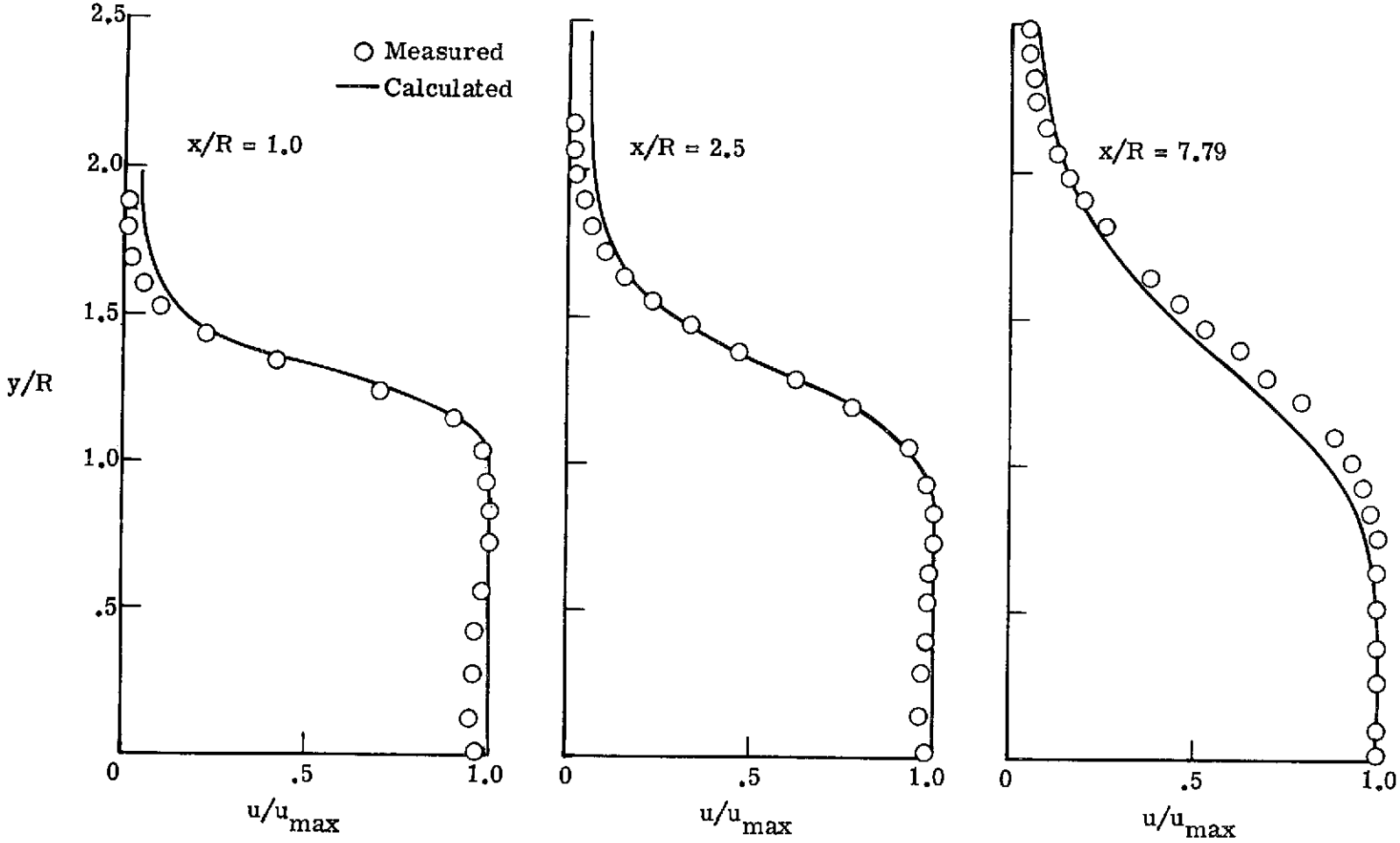

Figure 5.- Jet velocity profiles for Reynolds number of 600.

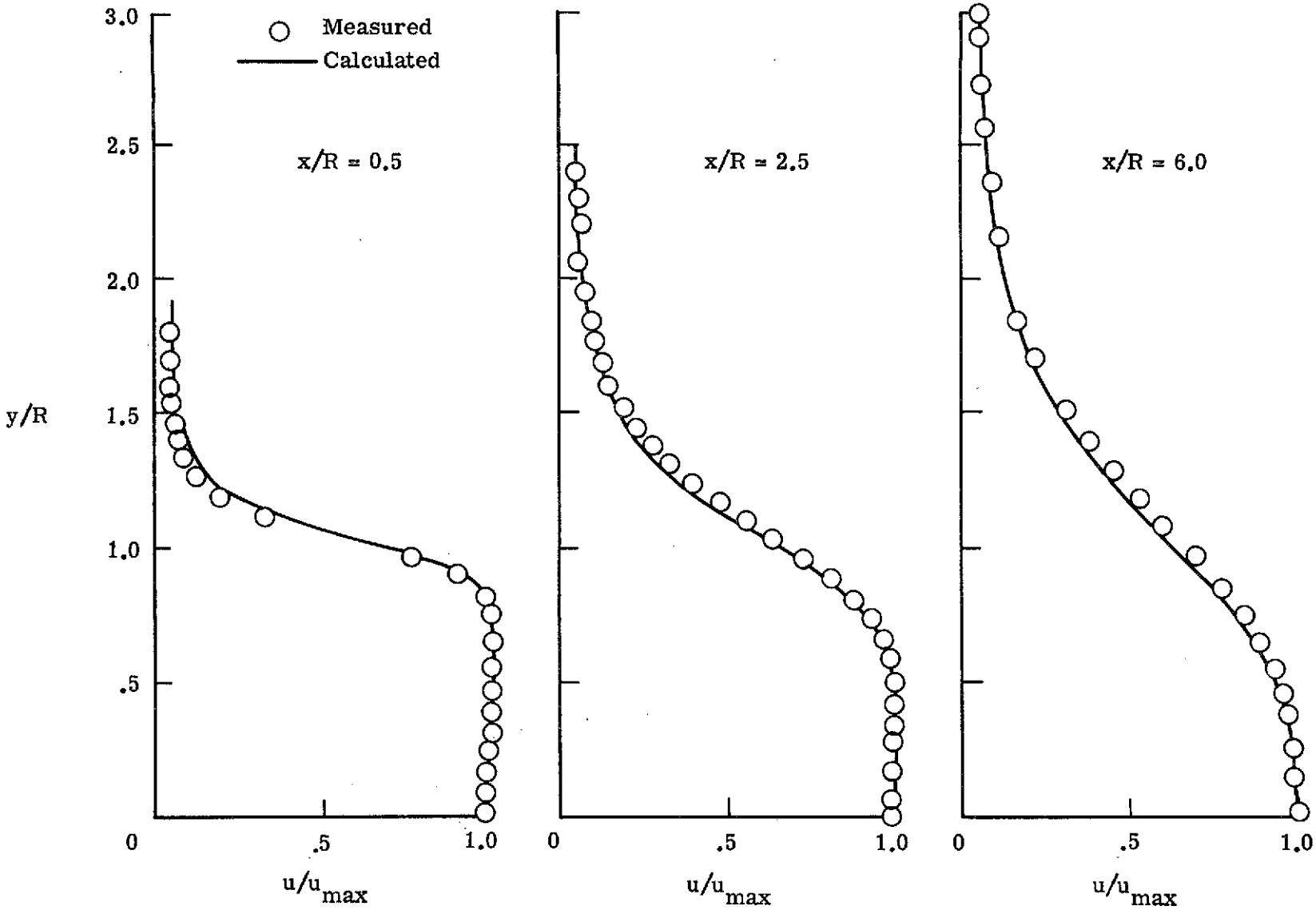

Figure 6.- Jet velocity profiles for Reynolds number of 200.

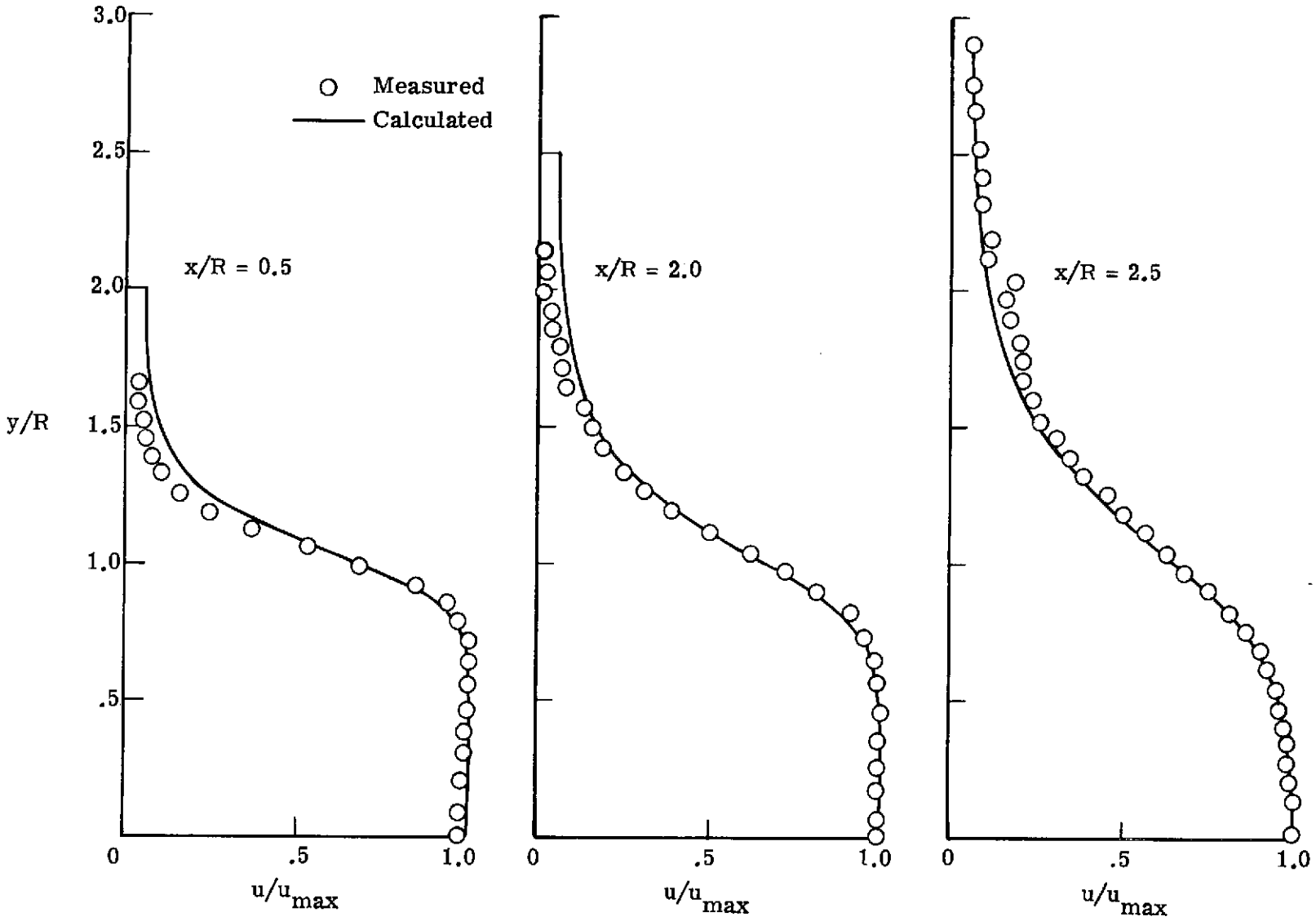

Figure 7.- Jet velocity profiles for Reynolds number of 100.

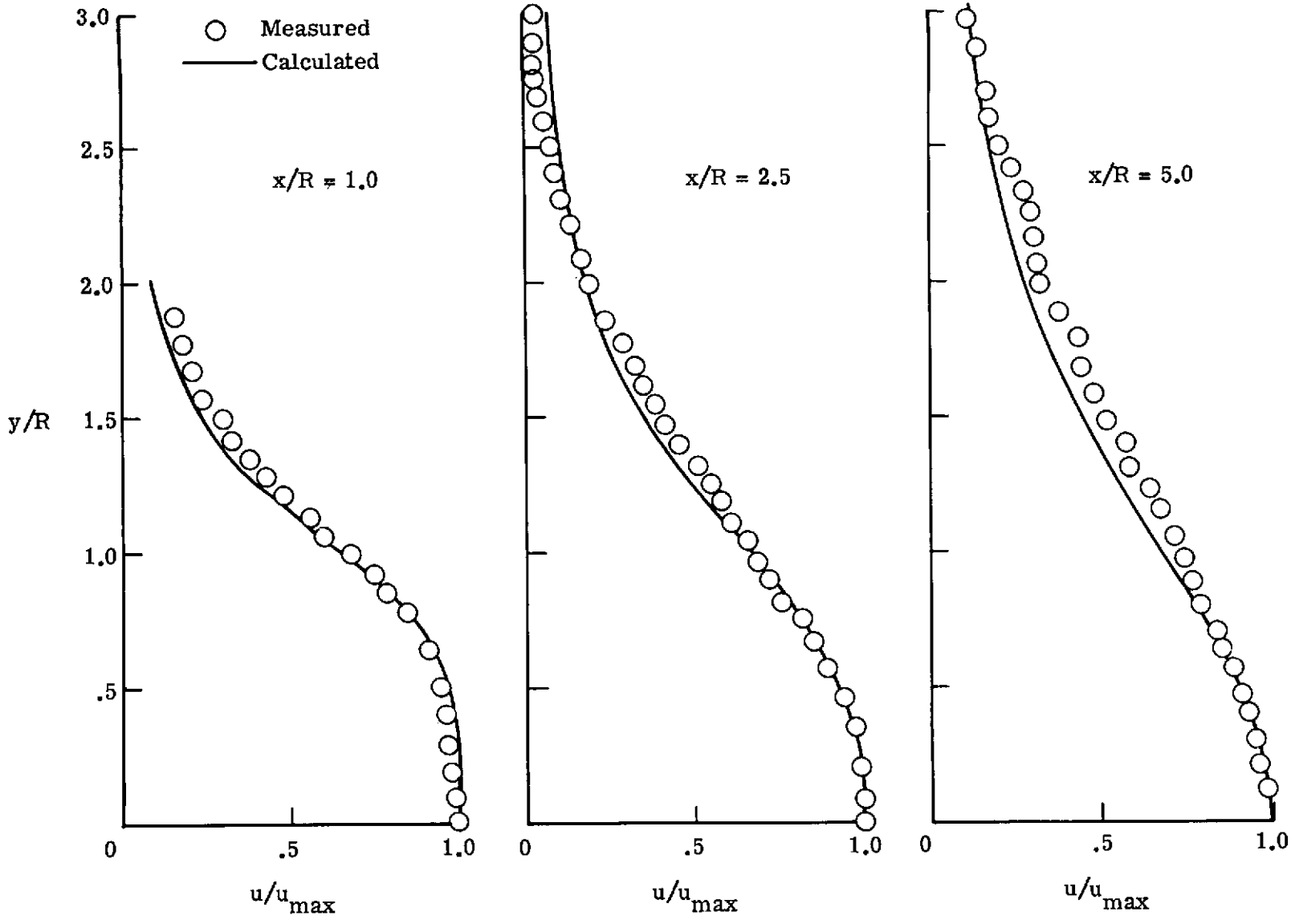

Figure 8.- Jet velocity profiles for Reynolds number of 50.

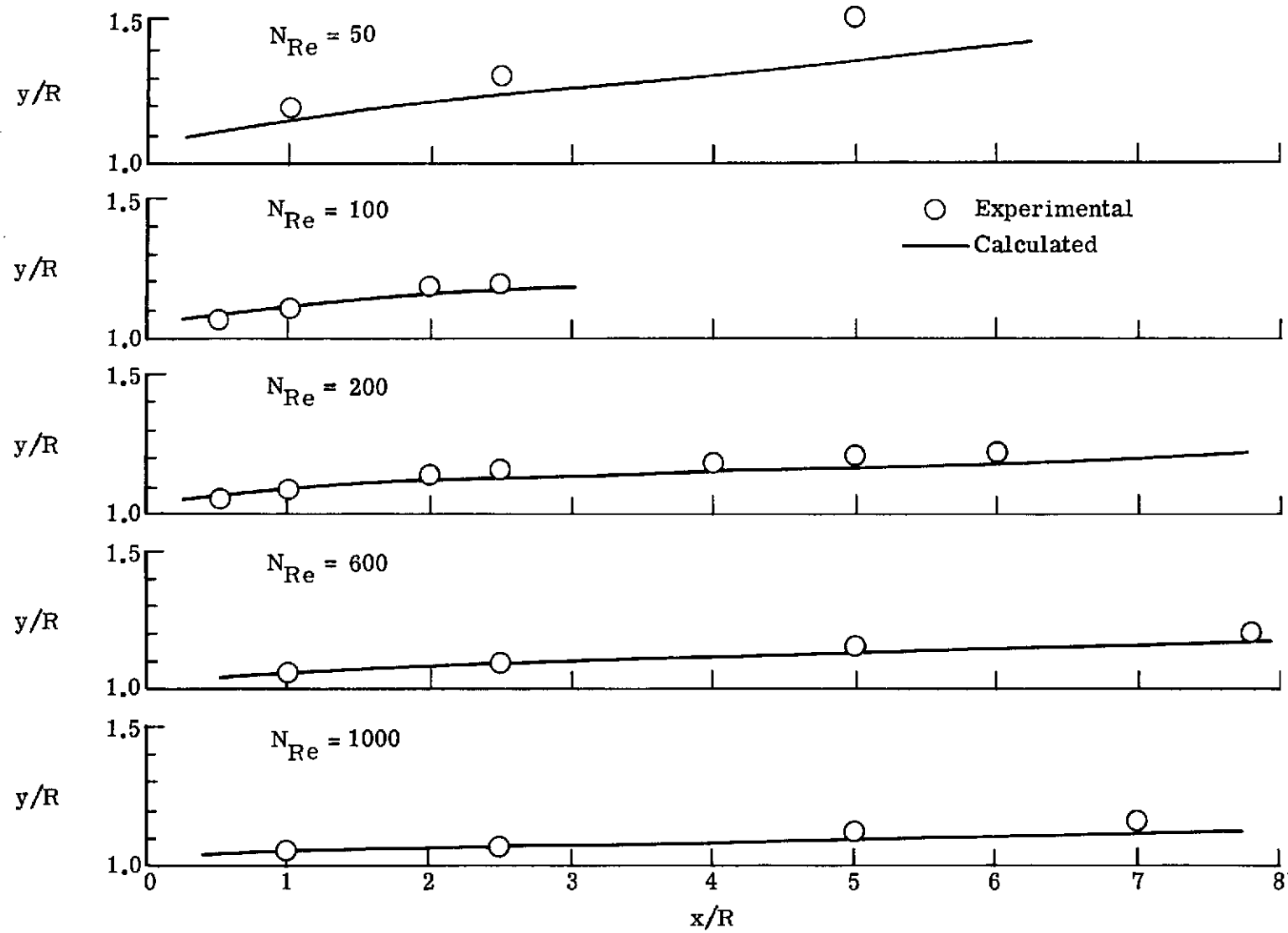

Figure 9.- Variation of the 0.5-velocity radius with x/R and Reynolds number.